Mathematical Modeling of PAG and NIPAM-Based Polymer Gel Dosimeters contaminated by oxygen and inhibitor.

Valeria I Koeva[1], Shahab Daneshvar[1], Robert J Senden[1], A H M Imam[1], L John Schreiner[2,3] and Kimberley B McAuley[1*]

[1] Department of Chemical Engineering, Queen's University, Kingston, ON, Canada, K7L 3N6

[2] Cancer Centre of Southeastern Ontario, Kingston, ON, Canada, K7L 5P9

[3] Departments of Oncology and Physics, Queen's University, Kingston, ON, Canada, K7L 3N6

E-mail: kim.mcauley@chee.queensu.ca

Keywords: inhibition, modelling, parameter estimation, polymer gel dosimetry, radiation, parameter estimation, oxygen

Abstract

A mathematical model for crosslinking copolymerization of acrylamide (or N-isopropyl acrylamide, NIPAM) and N,N'-methylene bisacrylamide is extended to account for contamination by oxygen and the inhibitor monomethyl ether hydroquinone (MEHQ). This model improves basic understanding of interactions among oxygen, MEHQ and polymerization reactions in gel dosimeters that are used to verify radiation doses delivered by cancer treatment equipment. Improved parameter estimates result in a good match between model predictions and data. The model predicts that the duration of the oxygen inhibition

period increases with increasing oxygen contamination, in agreement with experimental data. The model also predicts that MEHQ, in the absence of oxygen, has almost no influence on dosimeter response.

Introduction

Polymer gel dosimetry is a technique used by medical physicists to verify radiation dose distributions delivered by cancer radiotherapy equipment.[1] To test whether the correct radiation dose is being delivered to the correct location, a small polymerization vessel is irradiated instead of the patient. Radiation absorbed by water in the aqueous solution leads to generation of free radicals, which induce polymerization. The quantity of polymer that forms at different locations depends on the amount of radiation received at the particular location. The most widely used polymer gel dosimeter is the Polyacrylamide Gel (PAG) dosimeter. PAG dosimeter recipes consist of acrylamide (Aam) and N,N'-methylene-bisacrylamide (Bis) crosslinker dissolved in an aqueous gelatin matrix. In some dosimeters, Aam is replaced by N-isopropylacrylamide (NIPAM). Chemical structures for Aam, NIPAM and Bis are shown below. A typical recipe for a PAG dosimeter is shown in Table 1.

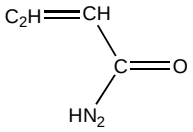

Aam

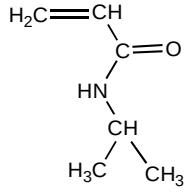

NIPAM

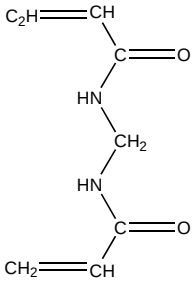

Bis

Polymer gel dosimeter recipes are usually referred to by the concentrations of monomers in the solution prior to irradiation. The specifications most commonly used are %T, the total mass percent of monomers (e.g., Aam plus Bis) in the gel system and %C, the mass percent of the monomer mixture that is crosslinker. The recipe in Table 1 with 3% monomer and 3% crosslinker is referred to as a 6 %T 50 %C dosimeter.

Upon irradiation of the dosimeter solution, water molecules dissociate into free radicals that can initiate polymerization and crosslinking.[2] The densely crosslinked polymer microgels[3] that form precipitate from the aqueous phase. These microgels, which are too large to diffuse through the gelatin matrix, provide a means for storing spatial information about the absorbed radiation dose. Figure 1 is a photograph of a non-uniformly-irradiated PAG dosimeter. The white spiral and spherical regions in dosimeter received higher radiation doses than the surrounding transparent region. Uniformly-irradiated calibration vials in Figure 2 show how the amount of crosslinked polymer that forms increases with absorbed radiation dose. Radiation doses are specified in units of Gray (Gy), where 1 Gy corresponds to 1 Joule of ionizing radiation delivered per kg of sample. Radiation-induced changes in several physical properties of the gel can be measured using a variety of imaging techniques including MRI (Magnetic Resonance Imaging)[4], optical scanning[5] and x-ray computed tomography.[6]

Unfortunately, Aam is a severe neurotoxin and suspected carcinogen.[7] Recently, Senden et al. showed that Aam can be successfully replaced with NIPAM, thereby reducing some of the safety concerns associated with handling of highly toxic chemicals in the clinical environment.[8] A typical calibration curve produced using a NIPAM-based dosimeter is shown in Figure 3, in which the NMR transverse relaxation rate (R_2), which can be measured locally using MRI, is plotted against the radiation dose. Dose sensitivity is the slope of the initial linear portion of an R_2 vs. dose plot. Large dose sensitivity enables accurate dose calibration and read-out.

Commercial monomer-grade NIPAM and other monomers (but not Aam) that have been used in polymer gel dosimeters[8] contain monomethyl ether hydroquinone (MEHQ) inhibitor to prevent polymerization during shipping and storage.

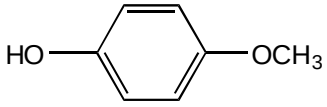

MEHQ

In polymer gel dosimeters, monomers are used without inhibitor removal, but the effect of MEHQ on polymerization kinetics and dose response in polymer gel dosimeters has not been studied. Oxygen, a well-known inhibitor of free-radical polymerization,[9,10] is another important contaminant in all polymer gel dosimeters, unless special precautions have been taken to remove it.[1] Oxygen contamination has a deleterious effect on the performance of polymer gel dosimeters.[11-13] Reactions between oxygen and free radicals are very fast, so that even small amounts of oxygen can consume enough radicals to significantly inhibit polymerization reactions. For example, when a dosimeter solution is initially in equilibrium with air, no appreciable polymerization (and no change in R_2) is observed until more than 20 Gy of radiation has been absorbed.[13] The level of O_2 contamination in polymer gel dosimeters can vary depending on manufacturing procedures and storage conditions prior to irradiation, resulting in variable dosimetry results. It is therefore important to reliably remove oxygen from polymer gel dosimeters. Traditionally this was done by bubbling the dosimeter solution with an inert gas,[14] but in recent years oxygen scavengers have been used to consume the dissolved O_2.[8,15-19] THPC is the preferred antioxidant due to its high reactivity in scavenging oxygen.[16] Dosimeters that contain antioxidants and are prepared in a fume hood under normal atmospheric conditions are referred to as "normoxic".

Previously, our research group developed two dynamic mathematical models[20,21] that describe the kinetic mechanisms of radiation-induced crosslinking copolymerization of Aam and Bis, using both spatially uniform and non-uniform radiation. Unfortunately, these models do not include the effects of oxygen or other inhibitors, assuming instead that all impurities have been removed from the dosimeter solution. The first model[20] uses the chemical mechanism in Table 2 to predict monomer and comonomer conversion, as well as the concentrations of crosslinks, unreacted pendant double bonds, and cyclized groups when radiation is absorbed uniformly throughout the reaction medium. Temperature rise due to exothermic polymerization reactions is also predicted. The second model,[21] with the same reaction mechanism, uses partial differential equations to account for the effects of spatially non-uniform radiation delivery (as in Figure 1).

Although the models were developed to simulate dosimeters that use Aam monomer, they are also useful for recipes that use NIPAM, since Aam and NIPAM have similar reaction rates due to their similar chemical structures. Note, however that the phase partitioning behaviours (between aqueous and polymer phases) of NIPAM and Aam may be quite different due to the isopropyl group on NIPAM. As shown in Table 2, the reaction steps included in the model are: radical generation by water radiolysis, initiation, propagation, cyclization, crosslinking, chain transfer to monomer, termination, chain transfer to gelatin and re-initiation. Phase separation and phase-volume changes due to crosslinking-induced precipitation and subsequent particle growth are also considered. These models have been particularly helpful in improving our understanding of "temporal instability" of polymer gel dosimeters, wherein long-lived radicals can persist in the dosimeter for several days after irradiation ceases, leading to ongoing polymerization and to associated changes in the R_2 vs. dose curve. The non-uniform radiation model[21] and a simplified model of DeDeene et al.[22] have been used to simulate the effects of sharp spatial gradients in radiation dose. As monomers are consumed in high-dose regions they begin to diffuse from regions of low dose to high dose. "Edge enhancement" occurs when diffusing monomers encounter radicals at the edge of the highly-irradiated region and polymerize there.

Unfortunately, some of the parameter values in these models[20, 21] are poorly known. Fuxman et al. used literature values for many of the rate constants in Table 2, but no published values were available for some of the kinetic and thermodynamic constants required in the model. Reactions with poorly-known rate constants are indicated by the symbol * on the reaction number in Table 2. Other model parameters that are poorly known are f (the initiation efficiency), D_{MI} (the diffusivity of acrylamide in the polymer phase) and v (the ratio of the reactivity of radicals with terminal Aam to the reactivity of radicals with terminal Bis). Trial-and-error simulations were used to select physically reasonable values of unknown parameters, resulting in a good qualitative match with experimental data available in the literature. Subsequently, new data[23] became available from dosimetry experiments involving recipes without gelatin, using a variety of radiation dose rates and total monomer concentrations. Unfortunately,

Fuxman's parameter values do not give good predictions of these gelatin-free gravimetric data, indicating that better parameter values are required so that the models can be used to simulate new recipes reliably.

New techniques have been developed to aid parameter estimation in complex polymerization models. Estimability analysis[24-26] is used to determine which parameters can be estimated from the available data, and which should remain at their initial values. Estimability analysis accounts for the structure of the model equations, for correlated effects of model parameters, and for the level of uncertainty in each of the initial parameter guesses. The algorithm, which produces a list of model parameters, ranked from most to least estimable has been used to determine which parameters can and should be estimated in models of other polymerization systems[24-27].

In the current article, the reaction mechanism in the spatially-uniform dosimeter model[20] is extended to account for the effects of oxygen and MEHQ contamination. Estimability analysis is then used to identify the poorly-known model parameters that can be estimated from the available gravimetric[23] data and calorimetric data with and without oxygen contamination[13]. Updated parameter values are obtained using the weighted-least squares estimation algorithm in Predici™, with the remaining parameters held at their literature values or the initial values of Fuxman et al. The extended model is then used to simulate the behaviour of PAG dosimeters that have been contaminated with oxygen and MEHQ. In the future, it will be important to include reactions involving THPC or other oxygen scavengers, so that the behaviour of normoxic polymer gel dosimeters can be simulated.

Extension of Mathematical Model to Include Oxygen and MEHQ Inhibition

Modeling of oxygen inhibition

We assume that oxygen inhibition takes place primarily in the aqueous phase, since the formation of the polymer phase is observed only after the inhibition period ends.[13] Oxygen can scavenge initiating (primary) radicals as well as propagating (polymer) radicals in polymer gel dosimeters. A similar oxygen

inhibition scheme has been used in models for the photopolymerization of acrylates.[28,29] Primary radicals produced by water radiolysis (Reaction 0 in Table 2) can react with dissolved oxygen. The resulting superoxide anion radicals ($O_2^{\bullet -}$) and perhydroxyl radicals ($HO_2^{\bullet}$) that form are unreactive toward most organic compounds and are therefore not expected to initiate polymerization.[30-32] The rate constants for radical-scavenging reactions between primary radicals and oxygen are of the same order of magnitude (~10^{10} $M^{-1}s^{-1}$) as the rate constants for initiation reactions between primary radicals and monomer. However, the total initial monomer concentration ($[M_i] \approx 0.6$ M) is much larger than the concentration of dissolved oxygen in air-saturated water at room temperature ($[O_2] \approx 2.5 \times 10^{-4}$ M). This large difference in the magnitude of the concentrations suggests that relatively few primary radicals are scavenged by oxygen. Instead, they propagate to form short polymer radicals. Hence, the main oxygen-inhibition mechanism is the scavenging of short propagating radicals, resulting in the formation of relatively stable organic peroxy radicals (Reactions 36 and 37 in Table 3).

Figure 4 shows that there is a competition between monomers and oxygen for propagating radicals. However, radical scavenging by O_2 is so fast (~5×10^8 $M^{-1}s^{-1}$)[29,33] compared to propagation (~1.5×10^4 $M^{-1}s^{-1}$ for AAm)[36] that the oxygen inhibition reactions are initially much faster than chain propagation even though $[O_2] << [M_i]$. Although propagation can occur, the polymerization rate is negligible until the oxygen concentration declines. For example, using the above rate constants and typical concentrations in a polymer gel dosimeter, the rates of oxygen scavenging and propagation finally become equal (i.e., $k[O_2] \approx k_p[M_i]$) when $[O_2]$ has decreased to less than 2×10^{-5} M (approximately 7-8% of the oxygen concentration for a dosimeter saturated with air). The effects of oxygen inhibition have been observed experimentally as an induction period (See Figure 7), with the length of the induction period depending on the level of oxygen contamination.[13]

The reaction mechanism in Figure 4 is shown in Table 3 using the notation of Fuxman et al.[20] wherein short oligomeric radicals of length *n* in the aqueous phase with terminal monomer *i* are given the symbol $S^w_{i,n}$. Subscripts i=1, 2 and 3 indicate that the terminal constituent on the polymeric radical is Aam, Bis or oxygen, respectively. As a result, R_n* in Figure 4 corresponds to $S_{1,n}{}^w$ or $S_{2,n}{}^w$ and R_n-O-O*

corresponds to $S_{3,n}^{w}$. The mechanism in Table 3 shows that peroxy radicals $S_{3,n}^{w}$ can react in three different ways: propagation (reactions 38 and 39), bimolecular termination (reactions 40-42) and hydrogen abstraction (chain transfer reactions 43 to 45). Since no visible polymer is produced in the presence of oxygen, the peroxy radicals must be relatively slow to propagate with monomers. Most peroxy radicals undergo rapid bimolecular termination,[35] or abstract protons from other molecules, e.g. monomers or gelatin.[36] The new radicals that form by hydrogen abstraction can again be scavenged by oxygen to produce new peroxy radicals. Decker and Jenkins used a similar mechanism to describe O_2 inhibition in the photopolymerization of multi-acrylates.[29]

Decker and Jenkins and Andrzejewska et al. reported rate constants for oxygen scavenging of polymer radicals on the order of 10^8-10^9 $M^{-1}s^{-1}$.[29,33] This approximate value is in agreement with very high ratios of oxygen inhibition rate constants to propagation rate constants elsewhere in the literature[37,38] Anseth et al. reported kinetic constants for methyl methacrylate, indicating that peroxy radicals (i.e., $S^{w}_{3,n}$) are 2 x 10^3 times less reactive towards monomer than are polymeric radicals.[39] Propagation rate constants for reactions of peroxy radicals with acrylamide and bisacrylamide, required for simulations in this article, were calculated using the propagation rate constant and the ratio $k_{p11}^{w} / k_{p31}^{w}$ = 2 x 10^3. Peroxy radicals are also assumed to be 2 x 10^3 times less reactive for chain transfer reactions than are polymeric radicals with a terminal monomer.

Since rate constants for the termination reactions of peroxy radicals in AAm/Bis systems are not available in the literature, they were approximated using data reported for (meth)acrylate polymerization. Kerber and Serini determined the rate constants for the re-initiation of peroxy radicals (k_{p31}) and bimolecular termination of two peroxy radicals (k_{t33}) for different free-radical polymerization systems in the presence of oxygen at 20 °C.[40] For methyl methacrylate the ratio k_{t33}/k_{p31} is approximately 10^7, which has been used in the current polymer gel dosimeter model. This value is in agreement with approximate rate constants for (meth)acrylate systems mentioned by Andrzejewska et al. [33]

The polyperoxides ($D_{3,n}$ in Table 3) and peroxy acids ($D_{4,n}$) that form in bimolecular termination and chain transfer reactions can decompose upon exposure to heat or light to form radicals that re-initiate

polymerization.[36] It is anticipated that irradiation of polymer gel dosimeters may also break the O-O bond to form additional radicals. However, these reactions are not included in the current model because the number of radicals formed in this manner will be much smaller than the number formed by water radiolysis, due to very high water concentrations.

Modeling of MEHQ inhibition

Commercial monomer-grade NIPAM contains about 500 ppm MEHQ. Phenolic inhibitors, such as MEHQ, require oxygen to function effectively[41], so that MEHQ is a less effective inhibitor in an oxygen-free environment than when oxygen is present. Several studies have focused on the role of oxygen and MEHQ and their synergistic interactions. Cutié et al. have shown that when MEHQ is added to acrylic acid polymerization systems, the rate of polymerization decreases but does not stop, indicating that MEHQ, by itself, is a retarder. [38] Cutié et al. also showed that when both MEHQ and oxygen are present, MEHQ can react with peroxy radicals to form stable radicals that can participate in termination reactions, but not in propagation reactions. Without MEHQ, some peroxy radicals eventually propagate with monomer, producing polymer chains with peroxy groups along the backbone.[42] MEHQ inhibits the formation and growth of polymer chains, reduces the consumption rate of oxygen, and enhances the inhibition by oxygen. Reactions involving MEHQ appear at the end of Table 3.

Since rate constants for inhibition reactions involving MEHQ in AAm/Bis or NIPAM/Bis systems are not available in the literature, we approximated them using data reported for acrylic acid polymerization.[38,43] We use ratios of kinetic rate constants determined by Cutie et al. for acrylic acid polymerization to make the following assumptions: i) the inhibition rate constants for reactions between MEHQ and polymeric radicals with terminal Aam and Bis units are $k_{inh,MEHQ1}=2.7 \times 10^{-5} k_{p11}$ and $k_{inh,MEHQ2}=2.7 \times 10^{-5} k_{p21}$, respectively; ii) the synergistic inhibition rate constant for reaction between MEHQ and a peroxy radical is $k_{inh,MEHQ3} = 200\ k_{p31}$ where k_{p31} is the rate constant for propagation of

peroxy radicals; iii) the rate constant for termination between an MEHQ radical and a peroxy radical is $k_{inh,MEHQ,4} = (10^4)k_{t33}$ where k_{t33} is the rate constant for bimolecular termination of two peroxy radicals.[40]

PREDICI® software was used to simulate the joint influence of MEHQ and oxygen using the reaction scheme shown in Table 3, along with the original reactions shown in Table 2. Peroxy radicals are relatively stable, but can react very quickly with MEHQ to form an even more stable radical Q_m* (reaction 48). This reaction accounts for the synergistic inhibition effects between oxygen and MEHQ. Peroxy radicals can combine rapidly in bimolecular termination reactions with the Q_m* radical. The products of the disproportionation reaction are oxygen molecules, which can further inhibit the polymerization, and dead species (reactions 49 and 50). In their model for MEHQ-inhibited polymerization of acrylic acid, Li and Schork[43] assumed that the Q_m* radicals cannot undergo any reactions except for termination with peroxy radicals, and we adopt a similar assumption. The rate of reaction of MEHQ with carbon-centered radicals is very slow (reactions 46 and 47) and the product radicals are very stable. As a result, we do not include the resulting Q* radicals in any subsequent reactions.

Estimability Analysis and Parameter Estimation

In this article, we estimate some of important but poorly-known parameters (see Table 4) that influence phase partitioning and reaction rates. During this analysis, other parameters, for which estimates are available in the literature, remain at their original values shown in Table 5. The improved parameter estimates are determined using gravimetric data from gelatin-free dosimeters[23] and calorimetric data[13] from typical PAG dosimeters containing gelatin. One calorimetry experiment was conducted on an oxygen-contaminated dosimeter, so the data set contains some information about oxygen-inhibition kinetics (See Figure 5). No calorimetric or gravimetric data are available for MEHQ-contaminated dosimeters, so none of the MEHQ-related parameters (values provided in Table 5) could be re-estimated. An initial attempt to estimate all 17 poorly-known parameters in Table 4 failed because the data set

contained insufficient information. As a result, some of the parameters have little influence on the predictions of the available data and the effects of some parameters are strongly correlated with the effects of other parameters, causing the parameter-estimation problem to be ill-conditioned.

To select an appropriate subset for estimation we used a parameter estimability algorithm[24-26] to rank the parameters from most estimable to least estimable. This algorithm requires initial guesses for all parameters, as well as information on the uncertainty associated with these guesses. Table 4 shows that the initial guess for k_{pg} is 0.008 L $mol^{-1}s^{-1}$ and that the initial uncertainty in this value is relatively large (0.05 L $mol^{-1}s^{-1}$). The relative uncertainty in k_{t11} is much smaller (2E8 L $mol^{-1}s^{-1}$, compared to an initial guess of 14.9E8 L $mol^{-1}s^{-1}$). The estimability algorithm selects k_{p13}, the rate constant for formation of peroxyradicals, as most estimable (ranked 1 in Table 4), because perturbations of this parameter from its initial guess (relative to the size of its initial uncertainty) have the largest overall influence on predictions of the available data. Successive parameters on the list were selected based on whether changes in their values (relative to their initial uncertainty) have large influences on model predictions and whether the effects of the parameters are correlated with those of parameters already selected.

After ranking all of the parameters, it is important to determine how many parameters can and should be estimated from the ranked list. The methodology used in this article is as follows. First, the most-estimable parameter (*i.e.,* k_{p13}) is estimated using the weighted nonlinear least-squares estimation algorithm in Predici® with all other parameters fixed at their initial guesses. Next, the top two parameters are estimated; then the top three, and so on. The objective function for parameter estimation and the qualitative fit of the model predictions to the data are examined after each iteration. Using this technique, we determined that reasonably good fits can be obtained after estimating the top eight parameters (shown in bold in Table 5) and that there is little improvement in the fit when additional parameters are estimated. When the model with the new parameter values is used to simulate dosimeter behaviour for a variety of different dose rates and recipes (i.e., different values of %C, %T and %gelatin), qualitative predictions

(not shown) are consistent with trends that have been observed experimentally[48-52] . A detailed summary of these trends is provided in Table 7 of the article of Fuxman et al.[20] Figure 5 shows the fits obtained for three calorimetric experiments used for parameter estimation. The model matches the data well, predicting a larger temperature rise (and more polymer formation) when the total radiation dose increases. The model is also able to predict the initial inhibition period for the oxygen-contaminated dosimeter irradiated to a total dose of 58.2 Gy. Figure 6 shows that the model can also predict the available gravimetric data for gelatin-free PAG dosimeters reasonably well. There is some mismatch at radiation doses below 5 Gy, with the model over-predicting the amount of polymer formed in the 2%T dosimeter and under-predicting the amount of polymer formed in the 6%T dosimeter.

Note that the predictions of the calorimetric data are only slightly better than the corresponding predictions obtained using the original parameters[20] because Fuxman et al. adjusted some of their unknown parameters manually to match these data. However, the new model parameters give much better predictions of the gravimetric data. Use of Fuxman's original parameter values to predict the mass of polymer formed in gelatin-free dosimeters (see Figure 6), results in simulations wherein less than 1 Gy of radiation results in essentially complete consumption of both Aam and Bis (not shown). However, the experimental data in Figure 6 reveal that a dose of more than 3 Gy is required to consume approximately half of the monomer. The new parameter values provide predictions that are consistent with this experimentally observed behaviour.

Examination of the parameter values in Table 4 reveals that many of final parameter estimates are similar in magnitude to the initial guesses. The parameters that changed the most are k_{t31} the rate constant for termination between peroxy radicals and propagating radicals (from 1E6 to ~2E3), k_{fg} the rate constant for propagation of gelatin-centred radicals (from 0.8 to 0.03) and Φ_{M1} the partition coefficient for monomer (from 0.6 to 0.088). Note that the estimability algorithm does not select influential parameters (e.g., the initiation efficiency *f*) for estimation when the modeler provides a relatively small uncertainty

value for the initial guess. The algorithm favours selection of parameters that the modeler has little prior knowledge about, with better-known parameters tending to appear near the bottom of the list.

Note that the value of 0.9299 obtained for the parameter θ (the fraction of gelatin-centered radicals that can initiate further polymerization (in Reactions 26 and 27 in Table 2) suggests that most or all of the radicals produced by chain-transfer to gelatin are capable of reinitiation reactions. Thus, the inhibiting influence of gelatin on the polymerization rate[18] can be explained by a slow initial propagation step ($k_{pg} << k_{p11}$) following chain-transfer to gelatin.

Using the extended model and improved parameter values, it is now possible to simulate the behaviour of PAG and related NIPAM-based dosimeters that have been contaminated with oxygen (and MEHQ). In the future, it will be important to include reactions involving THPC or other oxygen scavengers, so that the behaviour of normoxic polymer gel dosimeters can be simulated. When additional experimental data become available, it will be possible to incorporate more reactions in the model and to obtain improved parameter estimates.

Simulating the effects of oxygen and MEHQ inhibition

Figure 7 shows the predicted conversion of vinyl groups with different initial levels of oxygen in PAG dosimeters that are irradiated to a total dose of 20 Gy at a dose rate of 1 Gy/min. An induction period, in which very little polymerization occurs, is clearly observed in all of the simulated runs with oxygen. In these simulations, there is no appreciable conversion of vinyl groups until nearly all of the oxygen is consumed. The duration of the predicted induction period decreases when the amount of dissolved oxygen is decreased. These simulation results agree with experimental observations.[13]

Figure 8 shows the conversion of vinyl groups over time in dosimeters containing either oxygen or MEHQ, or both. Curve a) indicates that there is no noticeable inhibition when 15 ppm of MEHQ is present in the dosimeter, without oxygen. Note that 15 ppm of MEHQ in the final recipe corresponds to an MEHQ level of 500 ppm in the monomer, which is a typical amount in commercially-available

NIPAM. Curve b) shows that there is a short induction period when the dosimeter is contaminated by oxygen at a concentration of 2.5 x10^{-5} M, which is 10% of the concentration of O_2 in equilibrium with air (which is 2.5 x10^{-4} M). Curve c) shows an induction period of approximately 200 seconds when both MEHQ and oxygen are present. Comparison of curves b) and c) in Figure 8 shows that there is an appreciable change in the length of the induction period when MEHQ is added to an oxygen-contaminated dosimeter. The synergistic inhibition effect of oxygen and MEHQ becomes stronger as the oxygen concentration increases. In simulations where the concentration of O_2 in the dosimeter is in equilibrium with air (2.5 x10^{-4} M) and 15 ppm MEHQ is present, no appreciable polymerization is observed up to a total absorbed dose of 20 Gy, which requires 20 minutes of irradiation (results not shown). The results in Figure 8 demonstrate that MEHQ has no appreciable effect on the polymerization in the absence of oxygen, but it plays a significant role as an inhibitor when oxygen is present.

The simulation results in Figure 8 indicate that MEHQ contamination resulting from typical levels used in commercial-grade NIPAM have no appreciable influence on the rate of polymer formation in polymer gel dosimeters when all of the oxygen is scavenged from the system. Unfortunately, even small amounts of oxygen enhance the inhibiting effect of MEHQ to a point where no polymer is formed. As a result, scientists who manufacture and use polymer gel dosimeters need not take steps to remove MEHQ from the dosimeter solution. However, effective oxygen removal is essential to achieve reliable dosimeter results.

Conclusions

Reaction mechanisms for inhibition by oxygen and MEHQ were incorporated into a previous kinetic model for polyacrylamide gel dosimeters. Several important model parameters were estimated using gravimetric and calorimetric data, with and without oxygen contamination. Predictions obtained using the improved parameter values provide a reasonably good quantitative match to the experimental data used for parameter estimation. The oxygen inhibition observed in polymer gel dosimeters was successfully

modeled, based on the scavenging of propagating polymer radicals and the formation of relatively stable peroxy radicals. The model predicts an increase in the induction period with increasing levels of oxygen contamination. The model also predicts that MEHQ contamination, at typical levels associated with commercial NIPAM monomer, does not significantly influence the rate of polymerization and hence the dose response. However, when the effect of MEHQ is enhanced by the presence of oxygen in the system, significant inhibition occurs. As a result, it is recommended that dosimeter users should ensure that all oxygen is removed or chemically scavenged from dosimeter phantoms. However, MEHQ removal is not required. The extended model developed in this article is an important step toward predicting the behaviour of normoxic polymer gel dosimeters. Better understanding of the many chemical reactions involving the oxygen scavenger THPC is required before its influence can be included in mechanistic models in a meaningful way.

Acknowledgments

Funding for this work was provided by Natural Science and Engineering Research Council (NSERC), MITACS, the Canada Institutes of Health Research (CIHR), the Ontario Consortium of Image Guided Surgery and Therapy (OCITS), and Queen's University.

Nomenclature

a_i	mean distance travelled by a radical when an acrylamide (i=1) or bisacrylamide (i=2) monomer unit is added (m)
A	surface area of the vessel containing the PAG system [m^2]
C	cyclized unit
C_p	heat capacity of the PAG gel system [$J.g^{-1}.K^{-1}$]
D_n	dead polymer chain, for dead polymer chains formed by short radicals, the subscript n indicates the length of the chain
$D_{3,n}$	Dead polymer chain of length n, containing one or more peroxide groups
$D_{4,n}$	Dead polymer chain of length n, with a peroxy acid end group
DH	Hydrogen donor
D_{Mk}	diffusivity of acrylamide (k=1) or bisacrylamide (j=2) monomer in the polymer phase
$\dot{D}$	Rate at which the radiation is given [Gy. s^{-1}]
D_{Kj}	diffusivity in the polymer phase of a sort radical (K=S) or long crosslinked radical (K=L) bearing the active radical center on an acrylamide (j=1) or bisacrylamide (j=2) unit
e_{aq}^-	hydrated electron
f	radical efficiency
G	gelatin
G_i	chemical yield of specie i, where i can be $H^\bullet$, e_{aq}^- or $OH^\bullet$ [mol . J^{-1}]
$H^\bullet$	hydrogen radical
H_2	hydrogen molecule
H_2O_2	hydrogen peroxide molecule
H_2O^*	triplet excited water molecule
H_3O^+	oxonium ion

k_c^i rate constant for intramolecular cyclization reaction in the ith phase [s^{-1}]

$k_{f_{jk}}^i$ rate constant for transfer reaction in the ith phase between a macroradical bearing the active radical on an acrylamide unit (j=1) or bisacrylamide unit (j=2) and acrylamide monomer (k=1) or bisacrylamide monomer (k=2) [l . mol^{-1} . s^{-1}]

$k_{f_{Gj}}^i$ rate constant for transfer reaction in the ith phase between gelatin and a macroradical bearing the active radical on a acrylamide (j=1) or bisacrylamide (j=2) [l . mol^{-1} . s^{-1}]

$k_{p_{jk}}^i$ rate constant for propagation reaction in the ith phase between a macroradical bearing the active radical on a acrylamide (j=1) or bisacrylamide (j=2) and acrylamide (k=1) or bisacrylamide (k=2) monomer [l . mol^{-1} . s^{-1}]

$k_{p_{Gk}}^i$ rate constant for reaction in the ith phase between a gelatin radical and acrylamide (k=1) or bisacrylamide (k=2) monomer [l . mol^{-1} . s^{-1}]

$k_{t_{jk}}^i$ rate constant for termination reaction in the ith phase between a macroradical bearing the active radical on a acrylamide (j=1) or bisacrylamide (j=2) and a macroradical bearing the active radical on a acrylamide (k=1) or bisacrylamide (k=2) monomer [l . mol^{-1} . s^{-1}]

$k_{x_j}^i$ rate constant for reaction in the ith phase between a macroradical bearing the active radical on a acrylamide (j=1) or bisacrylamide (j=2) and an unreacted pendant double bond [l . mol^{-1} . s^{-1}]

$k_{p_{ij}}^o$ rate constant for propagation reactions in the absence of diffusion control [l . mol^{-1} . s^{-1}]

$k_{p_{ij}}^{diff}$ diffusion-limited rate constant for propagation reactions [l . mol^{-1} . s^{-1}]

$k_{t_{ij}}^o$ rate constant for termination reactions in the absence of diffusion control [l . mol^{-1} . s^{-1}]

$k_{t_{ij}}^{diff}$ diffusion-limited rate constant for termination reactions [l . mol^{-1} . s^{-1}]

L_p^i long crosslinked radical in the polymer phase bearing the active cite on a acrylamide (i=1), bisacrylamide (i=2) unit or on a newly crosslinked unit without a neighboring pendant double bond (i=3)

m mass of the gel system [kg]

M mass of irradiated water [kg]

M_1 acrylamide monomer

M_2 bisacrylamide monomer

n_{PDB} number of pendant double bonds on a water soluble polymer chain (growing radical or dead polymer chain)

n_C number of cyclized units on a water soluble polymer chain (growing radical or dead polymer chain)

N_A Avogadro's number

$OH^{\bullet}$ Hydroxyl radical

$O_2^{\bullet -}$ Superoxide anion radical

R* General notation for polymer radical

R-O-O* General notation for peroxy radical

R-O-O-R General notation for polyperoxide

R-O-OH General notation for peroxy acid

PDB_e un-reacted pendant double bond available for crosslinking

PDB_a un-reacted pendant double bond from the polymer phase available for crosslinking

$PR^{\bullet}$ primary radical

R_2 Transverse relaxation rate [s^{-1}]

r radii of interaction of free radicals

r_{db} rate of consumption of vinyl groups [$mol \cdot l^{-1} \cdot s^{-1}$]

R gas constant [1.9872 $cal \cdot mol^{-1} \cdot K^{-1}$]

$RPR^{\bullet}$ rate of generation of primary radicals [mol . s^{-1}]

S_{in}^{j} short radical with n monomer units, in the j^{th} phase, bearing the active cite on a acrylamide (i=1) or bisacrylamide (i=2) unit

T temperature in the PAG gel system [ºC]

T_s temperature of the surrounding environment [ºC]

v factor used to reduce the reactivity of radicals bearing the active site on a bisacrylamide unit

V^i volume of the i^{th} phase [l]

X crosslinked unit

Z typical length of the short radicals in the polymer phase

Superscripts

p polymer phase

w aqueous phase

• Designates a radical

Subscripts

n or *m* Number that indicated chain length

1 acrylamide

2 bisacrylamide

S short radical

L long radical

Greek Letters

σ Lennard-Jones diameter of the monomer

Φ ratio of the concentration of species in the polymerphase (^{p}) over the concentration of the same species in the aqueous phase (^{w})

γ gamma radiation

θ fraction of radicals on the gelatin that can re-initiate the polymerization

Symbols

ΔH_R Energy released per double bond consumed [kJ . mol^{-1}]

References

[1] M. J. Maryanski, R. J. Schulz, G. S. Ibbott, J. C. Gatenby, J. Xie, D. Horton and J. C. Gore, **1994b,** 'Magnetic resonance imaging of radiation dose distributions using a polymer-gel dosimeter', *Phys. Med. Biol.* **39** 1437-55.

[2] K. B. McAuley, **2004**, 'The chemistry and physics of polyacrylamide gel dosimeters: why they do and don't work', *Journal of Physics: Conference Series* **3**: 29-33.

[3] F. Teymour and J. D. Campbell, **1994**, 'Analysis of the dynamics of gelation in polymerization reactors using the "numerical fractionation" technique', *Macromolecules* 27, 2460–2469.

[4] J. C. Gore, Y. S. Kang and R. J. Schulz, **1984,** 'Measurement of radiation dose distributions by nuclear magnetic resonance (NMR) imaging', *Phys. Med. Biol.* **29** 1189-97.

[5] M. J. Maryanski, Y. Z. Zastavker and J. C. Gore, **1996a**, 'Radiation dose distributions in three dimensions from tomographic optical density scanning of polymer gels: II. Optical properties of the BANG polymer gel', *Phys. Med. Biol.* **41** 2705-17.

[6] M. Hilts, C. Audet, C. Duzenli and A. Jirasek, **2000**, 'Polymer gel dosimetry using x-ray computed tomography: a feasibility study', *Phys. Med. Biol.* **44** 2559-71.

[7] G. S. Ibbott, **2004**, 'Applications of gel dosimetry', *J. Phys.: Conf. Ser.* **3**, 58-77.

[8] R. J. Senden, P. De Jean, K. B. McAuley and L. J. Schreiner, **2006,** 'Polymer gel dosimeters with reduced toxicity: a preliminary investigation of the NMR and optical dose-response using different monomers', *Phys. Med. Biol.* **51** 3301-14

[9] A. Rudin **1982** 'The elements of polymer science and engineering', *Academic Press*, New York.

[10] G. Odian **1991** 'Principles of polymerization' *3rd ed* John Wiley & Sons, New York.

[11] S. J. Hepworth, M. O. Leach and S. J. Doran, **1999,** 'Dynamics of polymerization in polyacrylamide gel (PAG) dosimeters: (II) modelling oxygen diffusion', *Phys. Med. Biol.* **44** 1875-84.

[12] M. McJury, M. Oldham, M. O. Leach and S. Webb, **1999**, 'Dynamics of polymerization in polyacrylamide gel (PAG) dosimeters: (I) ageing and long-term stability', *Phys. Med. Biol.* **44** 1863-73.

[13] G. J. Salomons, Y. S. Park, K. B. McAuley and L. J. Schreiner, **2002**, 'Temperature increases associated with polymerization of irradiated PAG dosimeters', *Phys. Med. Biol.* **47** 1435-48.

[14] C. Baldock, R. P. Burford, N. Billingham, G. S. Wagner, S. Patval, R. D. Badawi, and S. F. Keevil, **1998**, 'Experimental procedure for the manufacture and calibration of polyacrylamide gel (PAG) for magnetic resonance imaging (MRI) radiation dosimetry', *Phys. Med. Biol.* **43** 695-702

[15] P. M. Fong, D. C. Keil, M. D. Does and J. C. Gore, **2001**, 'Polymer gels for magnetic resonance imaging of radiation dose distributions at normal room atmosphere', *Phys. Med. Biol.* **46** 3105-13.

[16] Y. De Deene, C. Hurley, A. Venning, K. Vergote, M. Mather, B. J. Healy and C. Baldock, **2002b**, 'A basic study of some normoxic polymer gel dosimeters', *Phys. Med. Biol.* **47** 3441-63.

[17] A. J. Venning, B. Hill, S. Brindha, B. J. Healy and C. Baldock, **2005**, 'Investigation of the PAGAT polymer gel dosimeter using magnetic resonance imaging', *Phys. Med. Biol.* **50** 3875-88.

[18] Y. De Deene, K. Vergote, C. Claeys and C. De Wagter, **2006**, 'The fundamental radiation properties of normoxic polymer gel dosimeters: a comparison between a methacrylic acid based gel and acrylamide based gels', *Phys. Med. Biol.* **51** 653-73.

[19] A. Jirasek, M. Hilts, C. Shaw and P. Baxter, **2006**, 'Investigation of tetrakis hydroxymethyl phosphonium chloride as an antioxidant for use in x-ray computed tomography polyacrylamide gel dosimetry', *Phys. Med. Biol.* **51** 1891-1906.

[20] A. M. Fuxman, K. B. McAuley and L. J. Schreiner, **2003**, 'Modeling of free-radical crosslinking copolymerization of acrylamide and N,N'-methylenebis(acrylamide) for radiation dosimetry', *Macromol. Theory Simul.* **12** 647-62.

[21] A. M. Fuxman, K. B. McAuley and L. J. Schreiner, **2005**, 'Modelling of polyacrylamide gel dosimeters with spatially non-uniform radiation dose distributions', *Chem. Eng. Sci.* **60** 1277-93.

[22] Y. De Deene, **2004**, 'Essential characteristics of polymer gel dosimeters', *J. of Phys.* **3** 34-57.

[23] S. Babic and L. J. Schreiner, **2006**, 'An NMR relaxometry and gravimetric study of gelatin-free aqueous polyacrylamide dosimeters', *Phys. Med. Biol.* **51**, 4171–4187.

[24] Z. K. Yao, B. M. Shaw, B. Kou, K. B. McAuley and D. W. Bacon, **2003**, "Modeling ethylene/butene copolymerization with multi-site catalyst: parameter estimability and experimental design", Polym. React. Eng. 11, 563-588.

[25] B. Kou, K. B. McAuley, C. C. Hsu, D. W. Bacon and K. Z. Yao, **2005, "**Mathematical model and parameter estimation for gas-phase ethylene homopolymerization with supported metallocene catalyst", Ind. Eng. Chem. Res., 44, 2428-2442.

[26] D. E. Thompson, K. B. McAuley and P. J. McLellan, **2009**, "Parameter estimation in a simplified molecular weight distribution model for HDPE produced by Ziegler-Natta catalyst", Macromol. React. Eng., published on-line.

[27] J. E. Puskas, S. Shaikh, K. Z. Yao, K. B. McAuley and G. Kaszas, **2005,** "Kinetic simulation of living carbocationic polymerization: simulation of living isobutylene polymerization using a mechanistic model", Eur. Polym. J., 41, 1-14.

[28] A. K. O'Brien and C. N. Bowman, **2006**, 'Modeling the effect of oxygen on photopolymerization kinetics' *Macromol. Theory Simul.* **15** 176-82.

[29] C. Decker and A. D. Jenkins, **1985**, 'Kinetic approach of O_2 inhibition in ultraviolet- and laser-induced polymerizations' *Macromolecules* **18** 1241-4.

[30] J. W. T. Spinks and R. J. Woods, **1976**, 'An Introduction to Radiation Chemistry' *2nd ed* John Wiley & Sons, New York.

[31] J. H. O'Donnell and D. F. Sangster, **1970**, 'Principles of radiation chemistry' *American Elsevier Publishing Company Inc*, New York.

[32] A. J. Swallow, **1973**, 'Radiation Chemistry' *Longman Group Limited*, London.

[33] E. Andrzejewska, M. B. Bogacki, M. A. Andrzejewski and M. Janaszczyk, **2003**, 'Termination mechanism during the photo-induced radical cross-linking polymerization in the presence and absence of oxygen' *Phys. Chem. Chem. Phys.* **5** 2635-42.

[34] J. Hernandez-Barajas and J. D. Hunkeler, **1997**, 'Inverse-emulsion polymerization of acrylamide using block copolymeric surfactants: mechanism, kinetics, and modeling', *Polymer* **38**(2) 437-447.

[35] M. H. George and A. Ghosh, **1978**, 'Effect of oxygen on the radical polymerization of acrylamide in ethanol and water' *J. Polym. Sci. Polym. Chem. Ed.* **16** 981-95.

[36] K. Kishore, V. Gayathri and K. Ravindran, **1981**, 'Formation and degradation of polymeric peroxides' *J. Macromol. Sci. Chem.* **A16 (8)** 1359-83.

[37] G. L. Batch and C. W. Macosko, **1990**, 'Oxygen inhibition in differential scanning calorimetry of free-radical polymerization' *Thermochim. Acta* **166** 185-98.

[38] S. S. Cutié, D. E. Henton, C. Powell, R. E. Reim, P. B. Smith and T. L. Staples, **1997**, 'The effects of MEHQ on the polymerization of acrylic acid in the preparation of superabsorbent gels' *J. Appl. Polym. Sci.* **64** 577-89.

[39] K. S. Anseth, S. M. Newman and C. N. Bowman, **1995**, 'Polymeric dental composites: properties and reaction behavior of multimethacrylate dental restorations' *Adv. Polym. Sci.* **122** 177-217.

[40] R. Kerber and V. Serini, **1970**, 'Bestimmung der wachtums- und abbruchskonstanten bei der copolymerisation von styrol, α-methylstyrol und methylmethacrylat mit molekularem sauerstoff' *Makromolekul. Chem.* **140** 1-19.

[41] L. B. Levy, **1985**, 'Inhibition of acrylic acid polymerization by phenothiazine and para-methoxyphenol' *J. Polym. Sci. Polym. Chem*. **23**, 1505-1515.

[42] J. J. Kurland, **1980**, 'Quantitative aspects of synergistic inhibition of oxygen and para-methoxyphenol in acrylic-acid polymerization' *J. Polym. Sci. Polym. Chem*. **18**, 1139-1145.

[43] R. Li and F. Joseph Schork, **2006**, 'Modeling of the Inhibition Mechanism of Acrylic Acid Polymerization' *Ind.Eng. Chem. Res.* **45**, 3001-3008.

[44] H. Tobita and A. E. Hamielec, **1990**, 'Crosslinking kinetics in polyacrylamide networks', *Polymer* **31** 1546-52.

[45] G. T Russell, D. H. Napper and R. G. Gilbert, **1988**, 'Termination in free-radical polymerizing systems at high conversion', *Macromolecules* **21**, 2133-40.

[46] R. C. Reis, J. M. Prausnitz and B. E. Poling, 'The Properties of Gases and Liquids', McGraw-Hill, New York **1987**.

[47] R. A. Orwoll, Y. S. Chong, in: Polymer Data Handbook, J. E. Mark, Ed., Oxford University Press, Oxford **1999**.

[48] M. J. Maryanski, C. Audet and J. C. Gore, **1997**, 'Effects of crosslinking and temperature on the dose response of a BANG polymer gel dosimeter', *Phys. Med. Biol.* **42**, 303-11.

[49] M. Lepage, A. K. Whittaker, L. Rintoul, and C. Baldock, **2001a**, '^{13}C-NMR, ^{1}H-NMR, and FT-Raman study of radiation-induced modifications in radiation dosimetry polymer gels', *J. Appl. Polym. Sci.* **79**, 1572-81.

[50] A. I. Jirasek and C. Duzenli , **2001**, 'Effects of crosslinker fraction in polymer gel dosimeters using FT Raman spectroscopy, *Phys. Med. Biol.* **46**, 1949-61.

[51] M. Lepage, A. K. Whittaker, L. Rintoul, S. Å. J. Bäck, and C. Baldock, **2001b**, 'The relationship between radiation-induced chemical processes and transverse relaxation times in polymer gel dosimeters', *Phys. Med. Biol.* **46**, 1061-74.

[52] C. Audet, **1995**, 'NMR-dose response studies of gels used for 3-D MRI radiation dosimetry', PhD Thesis, McGill University.

Tables:

Table 1: Typical 6%T, 50%C Polymer Gel Dosimeter Recipe.

Monomer	Acrylamide (AAm) or N-isopropylacrylamide (NIPAM)	3 g
Crosslinker	N,N'-methylene-bisacrylamide (Bis)	3 g
Gelatin		5 g
Water		89 ml
Antioxidant	Tetrakis (hydroxymethyl) phosphonium chloride (THPC)	10 mM

Table 2: PAG dosimeter reaction scheme developed by Fuxman et al.[20,21] Reaction numbers with a * indicate that the associated rate constant is poorly known.

Aqueous phase		Polymer phase (i=1, 2; j=1, 2)	
Radical generation			
Radiation $+H_2O \rightarrow (2PR^{\bullet w})$	(0)		
Initiation			
$(2PR^{\bullet w}) \xrightarrow{fast} f \cdot 2PR^{\bullet w}$	(1a)	$(2PR^{\bullet p}) \xrightarrow{fast} f \cdot 2PR^{\bullet p}$	(1b)
$2PR^{\bullet w} + M_1^w \xrightarrow{kini1} S_{1,1}^w$	(2a)	$2PR^{\bullet p} + M_1^p \xrightarrow{kini1} S_{1,1}^p$	(2b)
$2PR^{\bullet w} + M_2^w \xrightarrow{kini2} S_{2,1}^w$	(3a)	$2PR^{\bullet p} + M_2^p \xrightarrow{kini2} S_{2,1}^p$	(3b)
Propagation			
$S_{1,n}^w + M_1^w \xrightarrow{k_{p11}^w} S_{1,n+1}^w$	(4a)	$S_{i,n}^p + M_1^p \xrightarrow{k_{pi1,s}^p} S_{1,n+1}^p + (i\text{-}1)PDB_e^p$	(4b)
$S_{1,n}^w + M_2^w \xrightarrow{k_{p12}^w} S_{2,n+1}^w$	(5a)	$S_{i,n}^p + M_2^p \xrightarrow{k_{pi2,s}^p} S_{2,n+1}^p + (i\text{-}1)PDB_e^p$	(5b)
$S_{2,n}^w + M_1^w \xrightarrow{k_{p21}^w} S_{1,n+1}^w + PDB_e^w$	(6a)	$L_i^p + M_1^p \xrightarrow{k_{pi1,L}^p} L_1^p + (i\text{-}1)PDB_e^p$	(6b)
$S_{2,n}^w + M_2^w \xrightarrow{k_{p22}^w} S_{2,n+1}^w + PDB_e^w$	(7a)	$L_i^p + M_2^p \xrightarrow{k_{pi2,L}^p} L_2^p + (i\text{-}1)PDB_e^p$	(7b)
		$L_3^p + M_i^p \xrightarrow{k_{p2i,L}^p} L_i^p$	(8b)
Cyclization			
$S_{2,n}^w \xrightarrow{k_c^w} S_{1,n}^w + C^w$	(11a) *	$S_{2,n}^p \xrightarrow{k_c} S_{1,n}^p + C^p$	(11b)
		$L_2^p \xrightarrow{k_c} L_1^p + C^p$	(12b)
Crosslinking			
$S_{1,n}^w + PDB_e^w \xrightarrow{k_{x1}^w} S_{x,n}^w + X^w$	(13a)	$S_{1,n}^p + PDB_e^w \xrightarrow{k_{x1,S}^p} L_3^p + X^p + (i\text{-}1)PDB_e^p$	(13b)
$S_{2,n}^w + PDB_e^w \xrightarrow{k_{x2}^w} S_{x,n}^w + X^w + PDB_e^w$	(14a)	$L_i^p + PDB_e^w \xrightarrow{k_{xi,L}^p} L_3^p + X^p + (i\text{-}1)PDB_e^p$	(14b)
$S_{1,n}^w + PDB_a^w \xrightarrow{k_{x1}^w} S_{x,n}^w + X^w$	(15a)		
$S_{2,n}^w + PDB_a^w \xrightarrow{k_{x2}^w} S_{x,n}^w + X^w + PDB_e^w$	(16a)		

Transfer to monomer

$S_{1,n}^{w} + M_1^{w} \xrightarrow{k_{f11}^{w}} S_{1,1}^{w} + D_n^{w} + PDB_e^{w}$ (17a)

$S_{i,n}^{p} + M_1^{p} \xrightarrow{k_{fi1,S}^{p}} S_{1,1}^{p} + D_S^{p} + iPDB_e^{p}$ (17b)

$S_{1,n}^{w} + M_2^{w} \xrightarrow{k_{f12}^{w}} S_{2,1}^{w} + D_n^{w} + PDB_e^{w}$ (18a)

$S_{i,n}^{p} + M_2^{p} \xrightarrow{k_{fi2,S}^{p}} S_{2,1}^{p} + D_S^{p} + iPDB_e^{p}$ (18b)

$S_{2,n}^{w} + M_1^{w} \xrightarrow{k_{f21}^{w}} S_{1,1}^{w} + D_n^{w} + 2PDB_e^{w}$ (19a)

$L_i^{p} + M_1^{p} \xrightarrow{k_{fi1,L}^{p}} S_1^{p} + D_L^{p} + iPDB_e^{p}$ (19b)

$S_{2,n}^{w} + M_2^{w} \xrightarrow{k_{f22}^{w}} S_{2,1}^{w} + D_n^{w} + 2PDB_e^{w}$ (20a)

$L_i^{p} + M_2^{p} \xrightarrow{k_{fi2,L}^{p}} S_2^{p} + D_L^{p} + iPDB_e^{p}$ (20b)

Termination by disproportionation

$S_{1,n}^{w} + S_{1,r}^{w} \xrightarrow{k_{t11}^{w}} D_n^{w} + D_r^{w} + PDB_e^{w}$ (21a)

$S_{i,n}^{p} + S_{j,r}^{p} \xrightarrow{k_{tij,S}^{p}} D_n^{p} + D_r^{p} + (i+ j- 1)PDB_e^{p}$ (21b)

$S_{1,n}^{w} + S_{2,r}^{w} \xrightarrow{k_{t12}^{w}} D_n^{w} + D_r^{w} + 2PDB_e^{w}$ (22a)

$L_i^{p} + L_j^{p} \xrightarrow{k_{tij,L}^{p}} D_L^{p} + D_L^{p} + (\text{i+ j- 1})PDB_e^{p}$ (22b)

$S_{2,n}^{w} + S_{2,r}^{w} \xrightarrow{k_{t22}^{w}} D_n^{w} + D_r^{w} + 3PDB_e^{w}$ (23a)

$S_{i,n}^{p} + L_j^{p} \xrightarrow{k_{tij,SL}^{p}} D_n^{p} + D_L^{p} + (\text{i+ j- 1})PDB_e^{p}$ (23b)

Transfer to Gelatin

$S_{1,n}^{w} + G^{w} \xrightarrow{k_{fG1}^{w}} \theta G^{\bullet w} + D_n^{w}$ (24a)*

$S_{1,n}^{p} + G^{p} \xrightarrow{k_{fGi,S}^{p}} \theta G^{\bullet p} + D_n^{p} + (\text{i-1})\, PDB_e^{p}$ (24b)*

$S_{2,n}^{w} + G^{w} \xrightarrow{k_{fG2}^{w}} \theta G^{\bullet w} + D_n^{w} + PDB_e^{w}$ (25a)*

$L_i^{p} + G^{p} \xrightarrow{k_{fGi,L}^{p}} \theta G^{\bullet p} + D_L^{p} + (\text{i-1})\, PDB_e^{p}$ (25b)*

Re-Initiation of Gelatin Radicals

$G^{\bullet w} + M_1^{w} \xrightarrow{k_{pG1}^{w}} S_{1,1}^{w} + G^{w}$ (26a)*

$G^{\bullet p} + M_1^{p} \xrightarrow{k_{pG1}^{w}} L_1^{p} + G^{p}$ (26b)*

$G^{\bullet w} + M_2^{w} \xrightarrow{k_{pG2}^{w}} S_{2,1}^{w} + G^{w}$ (27a)*

$G^{\bullet p} + M_2^{p} \xrightarrow{k_{pG2}^{w}} L_2^{p} + G^{p}$ (27b)*

Transfer between phases

$S_{x,n}^{w} \xrightarrow{precip.} L_3^{p}$ (28)

$PDB_e^{p}, C^{w}, X^{w} \xrightarrow{precip.} PDB_e^{p}, C^{p}, X^{p}$ (29)

$M_1^{w} \overset{\Phi_{M1}}{\longleftrightarrow} M_1^{p}$ (30)*

$M_2^{w} \overset{\Phi_{M2}}{\longleftrightarrow} M_2^{p}$ (31)*

$H_2O^{w} \overset{\Phi_{H2O}}{\longleftrightarrow} H_2O^{p}$ (33)*

$G^{w} \overset{\Phi_{G}}{\leftrightarrow} G^{p}$ (34)

$PDB_{acc}^{w} \overset{\Phi_{PDB}}{\longleftrightarrow} PDB_{eff}^{p}$ (35)*

Table 3: Proposed reaction scheme for oxygen inhibition reactions and for reactions involving MEHQ.

Oxygen incorporation

$$S_{1,n}^{w} + O_2 \xrightarrow{k_{p13}} S_{3,n}^{w} \quad (36)$$

$$S_{2,n}^{w} + O_2 \xrightarrow{k_{p23}} S_{3,n}^{w} \quad (37)$$

Propagation of peroxy radicals

$$S_{3,n}^{w} + M_1^{w} \xrightarrow{k_{f31}^{w}} S_{1,1}^{w} + D_{4,n}^{w} \quad (38)$$

$$S_{3,n}^{w} + M_2^{w} \xrightarrow{k_{f32}^{w}} S_{2,1}^{w} + D_{4,n}^{w} \quad (39)$$

Termination of peroxy radicals

$$S_{3,n}^{w} + S_{1,m}^{w} \xrightarrow{k_{t31}^{w}} D_{4,n}^{w} + D_m^{w} + PDB_e^{w} \quad (40)$$

$$S_{3,n}^{w} + S_{2,m}^{w} \xrightarrow{k_{t32}^{w}} D_{4,n}^{w} + D_m^{w} + 2PDB_e^{w} \quad (41)$$

$$S_{3,n}^{w} + S_{3,m}^{w} \xrightarrow{k_{t33}^{w}} D_{3,n+m}^{w} + O_2 \quad (42)$$

Transfer to monomers and gelatin by peroxy radicals

$$S_{3,n}^{w} + M_1^{w} \xrightarrow{k_{p31}^{w}} S_{1,n+1}^{w} \quad (43)$$

$$S_{3,n}^{w} + M_2^{w} \xrightarrow{k_{p32}^{w}} S_{2,n+1}^{w} \quad (44)$$

$$S_{3,n}^{w} + G \xrightarrow{k_{f3G}^{w}} D_{4,n}^{w} + G^{\bullet} \quad (45)$$

Termination with MEHQ

$$S_{1,n}^{w} + \text{MEHQ} \xrightarrow{k_{inh,MEHQ1}} Q^{*} \quad (46)$$

$$S_{2,n}^{w} + \text{MEHQ} \xrightarrow{k_{inh,MEHQ2}} Q^{*} \quad (47)$$

Synergistic inhibition of peroxy radicals by MEHQ

$$S_{3,n}^{w} + \text{MEHQ} \xrightarrow{k_{inh,MEHQ3}} Q_m^{*} \quad (48)$$

Synergistic termination of peroxy radicals

$$S_{3,n}^{w} + Q_m^{*} \xrightarrow{k_{inh,MEHQ4}} Q_{n+m}^{w} + O_2 \quad (49)$$

$$S_{3,n}^{w} + Q_m^{*} \xrightarrow{k_{inh,MEHQ4}} Q_n^{w} + Q_m^{w} + 2O_2 \quad (50)$$

Table 4: Parameter estimates and estimability ranking for poorly known parameters.

Parameter	Description	Units	Estimability Ranking	Initial Guess	Guess Uncertainty	Final Estimate
k_{p13}	Rate constant for formation of a peroxy radical	$M^{-1}s^{-1}$	1	5.0E+08	4.0E+08	2.04E+08
k_{pg}	Propagation of gelatin-centred radicals	$L\ mol^{-1}\ s^{-1}$	2	0.008	0.05	3.676E-03
Φ_{H2O}	Partition coefficient for water between polymer and aqueous phases	$\frac{mol/L_{pol}}{mol/L_{aq}}$	3	0.9	0.3	0.682
k_{fg}	Chain transfer to gelatin	$L\ mol^{-1}\ s^{-1}$	4	0.8	2.0	2.83E-02
θ	Fraction of gelatin-centred radicals that can propagate		5	0.8	0.2	0.9299
k_{t31}	Rate constant for termination reaction between a polymer radical bearing the active radical on a peroxy unit and a polymer radical bearing the active radical on an acrylamide unit	$M^{-1}s^{-1}$	6	1.0E+06	2.0E+06	2.38E+03
Φ_{M1}	Partition coefficient for monomers between polymer and aqueous phases	$\frac{mol/L_{pol}}{mol/L_{aq}}$	7	0.6	0.3	0.0881
Φ_{PDB}	Fraction of pendant vinyl groups in polymer phase that can crosslink with aqueous-phase radicals		8	0.1	0.1	
k_c	Primary cyclization	s^{-1}	9	6.0E+04	3.0E+04	1.15E+04
f	Radical efficiency in aqueous phase		10	0.5	0.1	
D_{M1}	Diffusivity of acrylamide in polymer phase	$m^2\ s^{-1}$	11	1.0E-11	1.0E-12	
ν	Ratio of reactivity of radicals with terminal acrylamide to radicals with bisacrylamide		12	2	0.5	
k_{p11}	Propagation rate coefficient in the absence of diffusion control.	$L\ mol^{-1}s^{-1}$	13	1.65E+06	2.0E+05	
h	Heat transfer coefficient for heat transfer from the PAG to the surrounding environment.	$Jcm^{-2}K^{-1}s^{-1}$	14	5.0E-03	5.0E-04	
k_{t11}	Bimolecular termination rate coefficient in the absence of diffusion control.	$L\ mol^{-1}s^{-1}$	15	1.41E+09	2.0E+08	
k_{f11}	Rate coefficient for transfer reaction between a macroradical and monomer.	$L\ mol^{-1}s^{-1}$	16	9.55E+06	9.55E+06	
k_{i3}	Rate constant for inhibition reaction between primary radicals and oxygen.	$M^{-1}s^{-1}$	17	1.0E+10	1.0E+10	

Table 5: Parameters required for Polymer Gel Dosimeter Simulations. The parameters that are in **bold** are new values estimated from experimental data.[13,23] The remaining values were used by Fuxman et al.[20,21] or are from the literature.

Parameter	Value	Description	Units	Source
a) Model parameters for simulations without oxygen and MEHQ				
k_{ini_1}	$\approx 1 \times 10^{10}$	Initiation rate constant for reaction between primary radical and monomer.	L mol^{-1}s^{-1}	[30]
$k^0_{p_{11}}$	1.65×10^6 *exp* (-2743/RT)	Propagation rate coefficient in the absence of diffusion control.	L mol^{-1}s^{-1}	[34]
$\boldsymbol{k_{pg}}$	**3.676E-03**	Propagation of gelatin-centred radicals	L mol^{-1}s^{-1}	
$k^0_{f_{11}}$	9.55×10^6 *exp* (-10438/RT)	Rate coefficient for transfer reaction between a macroradical and monomer.	L mol^{-1}s^{-1}	[34]
$\boldsymbol{k_{fg}}$	**0.02825**	Chain transfer to gelatin	L mol^{-1} s^{-1}	
$k^0_{t_{11}}$	(1532 *exp* (-741/RT))^2	Bimolecular termination rate coefficient in the absence of diffusion control.	L mol^{-1}s^{-1}	[34]
$\boldsymbol{k_c}$	**1.1495E+04**	Primary cyclization	s^{-1}	
$k^0_{p_{11}}/k^o_{p_{12}}$	0.5		-	[44]
$k^0_{p_{22}}/k^0_{p_{21}}$	2		-	[44]
$\boldsymbol{\theta}$	**0.929993**	Fraction of gelatin-centred radicals that can propagate		
σ_{M_1}	5.02×10^{-8}	Lennard-Jones diameter of acrylamide monomer.	cm	[45,46]
σ_{M_2}	6.42×10^{-8}	Lennard-Jones diameter of bisacrylamide monomer.	cm	[45,46]
a_1	1.54×10^{-8}	Mean distance travelled by a radical when an acrylamide monomer unit is added.	cm	[47]
$D_{M_1^w}$	4×10^{-6}	Diffusivity in the water phase of acrylamide monomer.	cm^{2}s^{-1}	[20]
$D_{H_2O^w}$	1.5×10^{-5}	Diffusivity in the water phase of water.	cm^{2}s^{-1}	[20]
C_p	4184	Heat capacity of the PAG gel system.	Jkg^{-1}K^{-1}	[13]
$-\Delta H_R$	81500	Enthalpy of the reaction.	Jmol^{-1}	[34]
$k^{20°C}_{cond}$	5.98×10^{-3}	Thermal conductivity in the PAG gel dosimeter at 20°C.	Jcm^{-1}K^{-1}s^{-1}	[20]
h	5×10^{-3}	Heat transfer coefficient for heat transfer from the PAG to the surrounding environment.	Jcm^{-2}K^{-1}s^{-1}	[13]
$G_{(e^-_{aq}+H^\bullet+OH^\bullet)}$	6.27×10^{-7}	Chemical yield of $H^\bullet$, e^-_{aq} or $OH^\bullet$	molJ^{-1}	[20]
Φ_{PDB}	0.1	Fraction of pendant vinyl groups in polymer phase that can crosslink with aqueous-phase radicals.	-	[20]

Φ_{H_2O}	**0.6817**	Partition coefficient for water between polymer and aqueous phases	$\frac{mol/L_{pol}}{mol/L_{aq}}$	
Φ_M	**0.0881**	Partition coefficient for monomers between polymer and aqueous phases	$\frac{mol/L_{pol}}{mol/L_{aq}}$	
f	0.5	Radical efficiency in aqueous phase.	-	[20]
D_{M_1}	1.0E-11	Diffusivity of acrylamide in polymer phase.	$cm^2\ s^{-1}$	[20]
D_{M_2}	$3/4 D_{M_1}$	Diffusivity of bisacrylamide in polymer phase.	$cm^2\ s^{-1}$	[20]
$k_{x_1}^0$	$k_{p_{11}}^0$	Rate constant for reaction between a macroradical bearing the active radical on a acrylamide unit and un-reacted double bond.	$L\ mol^{-1}s^{-1}$	[20]
D_{PR^w}	$10 D_{M_1^w}$	Dead primary radicals in the aqueous phase.	$cm^2\ s^{-1}$	[20]
$D_{S_1^w}$	Varied from $D_{M_1^w}$ to 0	Dead polymer chain bearing the active radical on an acrylamide unit.	$cm^2\ s^{-1}$	[20]
$D_{S_2^w}$	$D_{S_1^w}$	Dead polymer chain bearing the active radical on a bisacrylamide unit.	$cm^2\ s^{-1}$	[20]
a_2	$2a_1$	Mean distance travelled by a radical when a bisacrylamide monomer unit is added.	cm	[20]
Φ_G	1	Ratio of the concentration of gelatin in the polymer phase over its concentration in aqueous phase.	-	[20]
ν	2	Ratio of reactivity of radicals with terminal acrylamide to radicals with bisacrylamide	-	[20]
b) Parameters for Reactions Involving Oxygen and MEHQ				
$k_{p_{13}}$	**2.04E+08**	Rate constant for inhibition reaction between oxygen and a polymer radical on an acrylamide unit	$M^{-1}s^{-1}$	
$k_{p_{23}}$	$k_{p_{13}}/\nu$	Rate constant for inhibition reaction between oxygen and a polymer radical on a bisacrylamide unit	$M^{-1}s^{-1}$	[20]
$k_{p_{21}}$	$\frac{k_{p_{11}}}{2000}$	Rate constant for re-initiation of a peroxy radical with acrylamide monomer	$M^{-1}s^{-1}$	[39]
$k_{p_{22}}$	$2k_{p_{21}}$	Rate constant for re-initiation of a peroxy radical with bisacrylamide monomer	$M^{-1}s^{-1}$	[20]
$k_{t_{23}}$	$k_{p_{21}} * 10^7$	Rate constant for termination reaction between a polymer radical bearing the active radical on a peroxy unit and a polymer radical bearing the active	$M^{-1}s^{-1}$	[40]

		radical on a peroxy unit		
$k_{t_{31}}$	**2.382E+03**	Rate constant for termination reaction between a polymer radical bearing the active radical on a peroxy unit and a polymer radical bearing the active radical on an acrylamide unit	$M^{-1}s^{-1}$	
$k_{t_{32}}$	$k_{t_{31}}/\nu$	Rate constant for termination reaction between a polymer radical bearing the active radical on a peroxy unit and a polymer radical bearing the active radical on a bisacrylamide unit	$M^{-1}s^{-1}$	[20]
$k_{f_{31}}$	$k_{f_{11}}$ /2000	Rate constant for chain transfer reaction of a polymer radical bearing the active radical on a peroxy unit to acrylamide monomer	$M^{-1}s^{-1}$	[40]
$k_{f_{32}}$	$2k_{f_{31}}$	Rate constant for chain transfer reaction of a polymer radical bearing the active radical on a peroxy unit to bisacrylamide monomer	$M^{-1}s^{-1}$	[20]
$k_{f_{3G}}$	$k_{f_{1G}}$ /2000	Rate constant for chain transfer reaction of a polymer radical bearing the active radical on a peroxy unit to gelatin	$M^{-1}s^{-1}$	[40]
$k_{inh,MEHQ_1}$	2.7E-05 ($k_{p_{11}}$)	Rate constant for the MEHQ-alone inhibition in case we have acrylamide unit at the end of the polymer chain.	$M^{-1}s^{-1}$	[38,43]
$k_{inh,MEHQ_2}$	2.7E-05 ($k_{p_{21}}$)	Rate constant for the MEHQ-alone inhibition in case we have bisacrylamide unit at the end of the polymer chain.	$M^{-1}s^{-1}$	[38,43]
$k_{inh,MEHQ_3}$	200 ($k_{p_{31}}$)	Rate constant determining the synergistic inhibition effect of oxygen and MEHQ.	$M^{-1}s^{-1}$	[38,43]
$k_{inh,MEHQ_4}$	$(10^4)k_{t_{33}}$	Rate coefficient describing the inhibition of the peroxy radicals by MEHQ radicals.	$M^{-1}s^{-1}$	[38,43]

Figures:

Figure 1: Photograph of a non-uniformly irradiated polymer gel dosimeter.

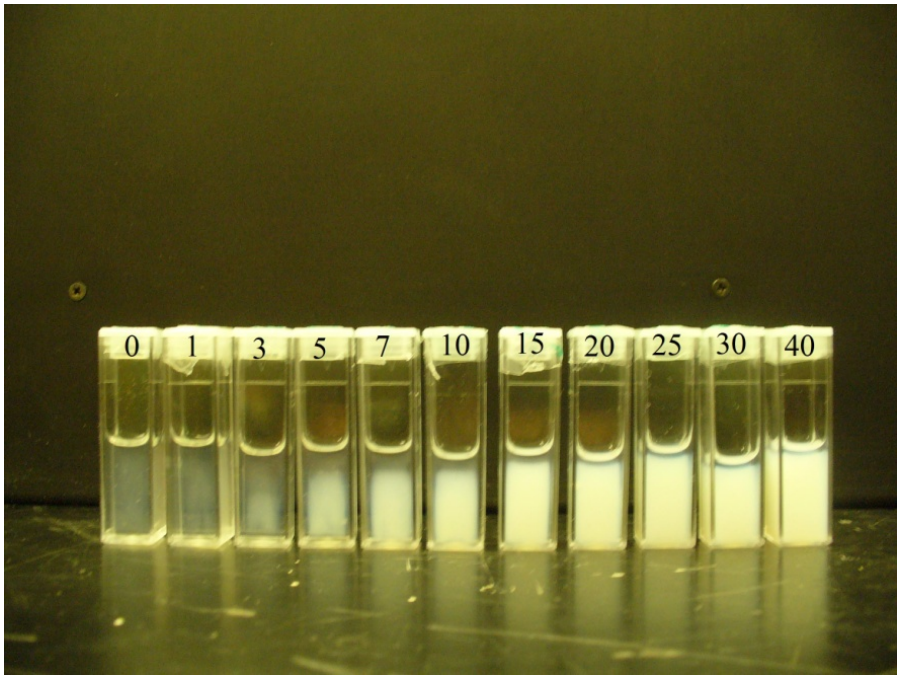

Figure 2: Photograph of uniformly-irradiated polymer gel dosimeters. Radiation doses vary from 0 Gy for the vial at the left to 40 Gy for the vial at the right.

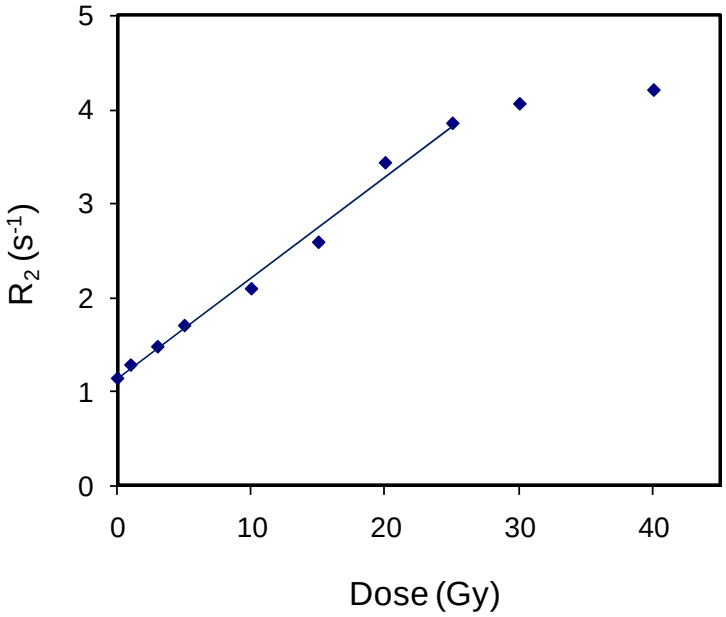

Figure 3: Dose-response curve of 6%T, 50%C NIPAM/Bis Dosimeter (♦)

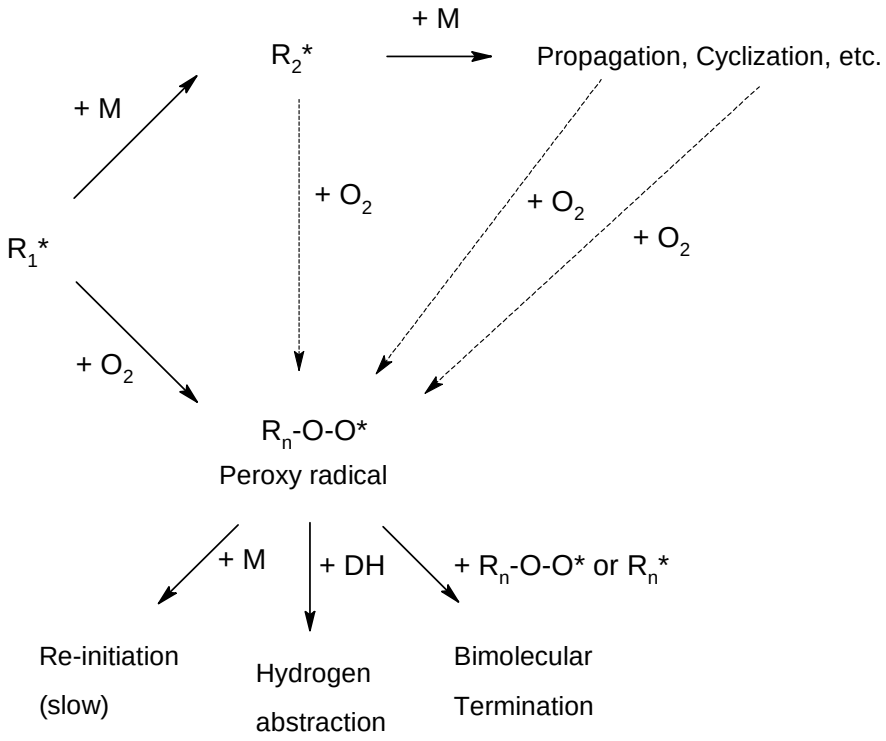

Figure 4: Reaction mechanism for oxygen inhibition by scavenging of propagating radicals. R_n* is a propagating chain of length n, R_n-O-O* is a polymeric chain of length n with a peroxy end unit, M is monomer and DH is a hydrogen donor such as monomer or gelatin that can participate in a chain-transfer reaction.[37]

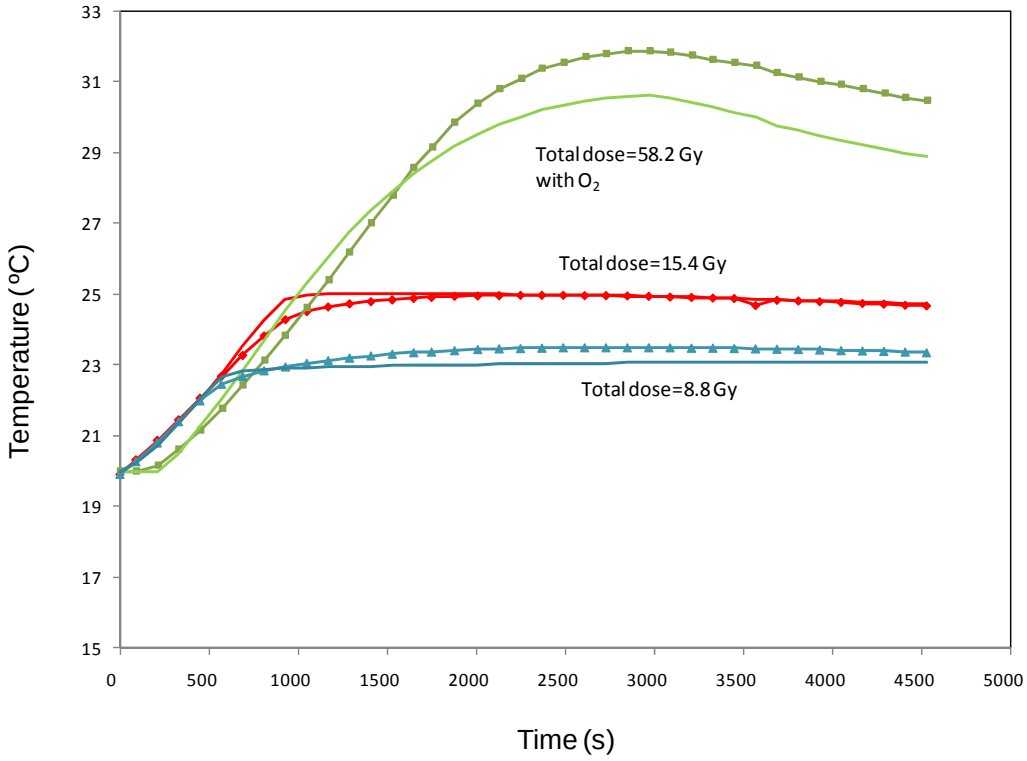

Figure 5: Comparison of simulated (—) and experimental (symbols) calorimetric data[13] obtained for 6 %T 50 %C PAG dosimeters. The dosimeters without oxygen were irradiated at a dose rate of 1.1 Gy/min to a total dose of 8.8 and 15.4 Gy, respectively. The oxygen-contaminated dosimeter was irradiated at a dose rate of 1.25 Gy/min to a total dose of 58.2 Gy.

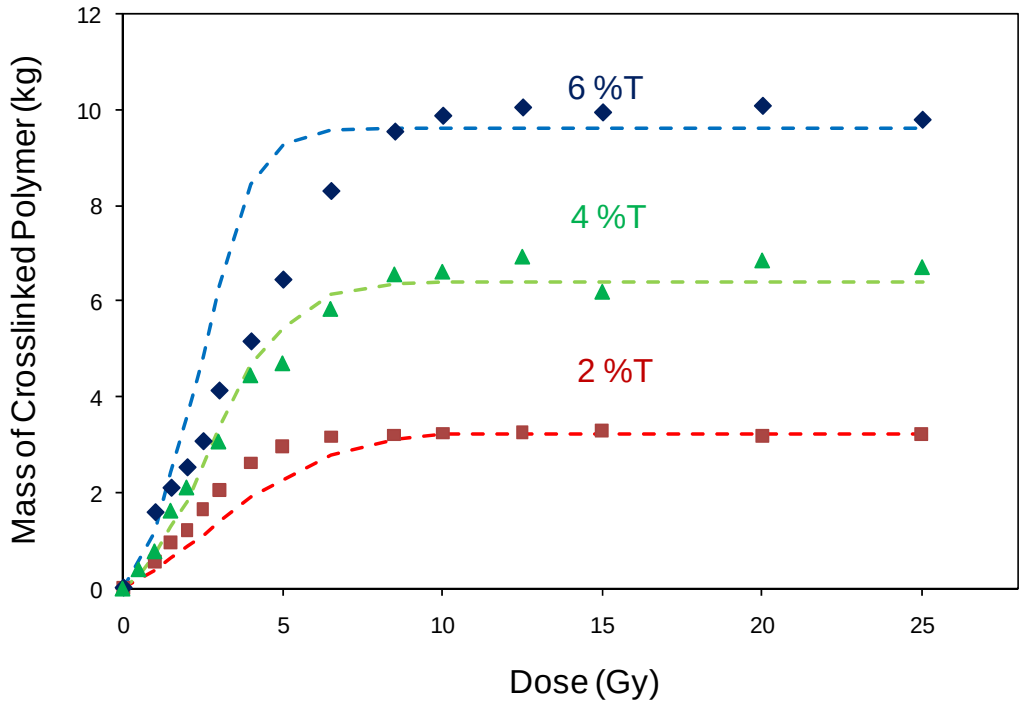

Figure 6: Comparison of simulated (-----) and experimental (symbols) gravimetric data[23] obtained for gelatin-free 50 %C PAG dosimeters irradiated at 1 Gy/min. Simulations were performed using parameter estimates from Table 4.

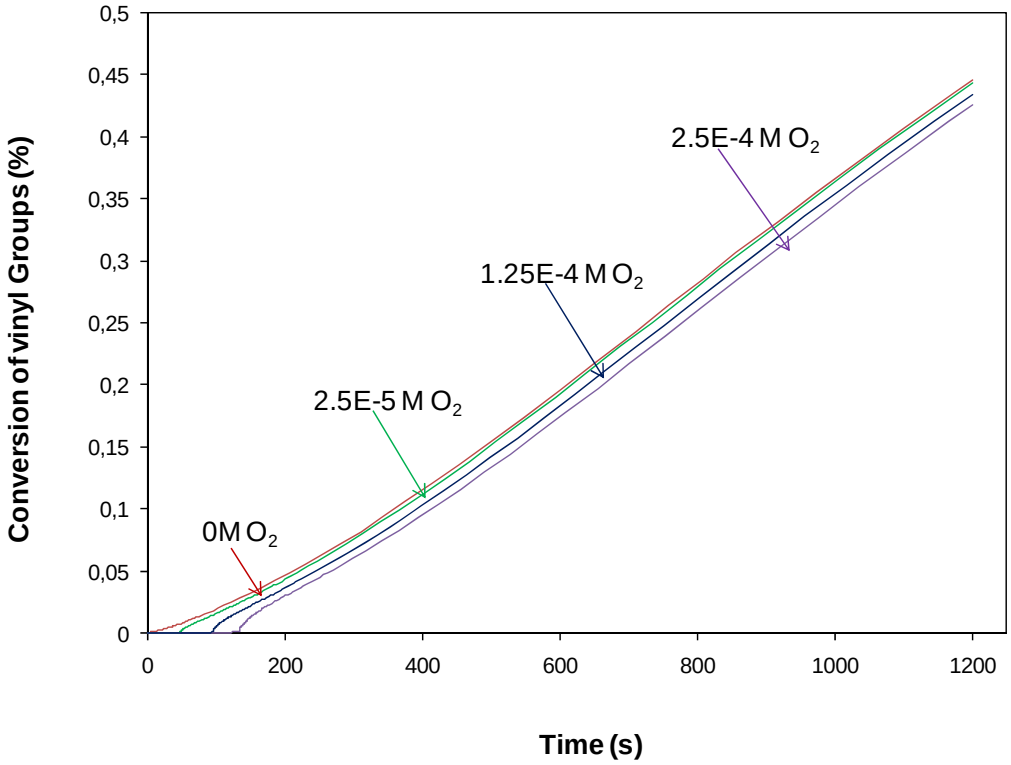

Figure 7: Simulation results showing the conversion of vinyl groups in PAG dosimeters with different initial concentrations of oxygen. The 6 %T, 50 % C dosimeters were irradiated at a dose rate of 1 Gy/min to a total dose of 20 Gy. The concentration of O_2 in a dosimeter in equilibrium with air is 2.5 $x10^{-4}$ M.

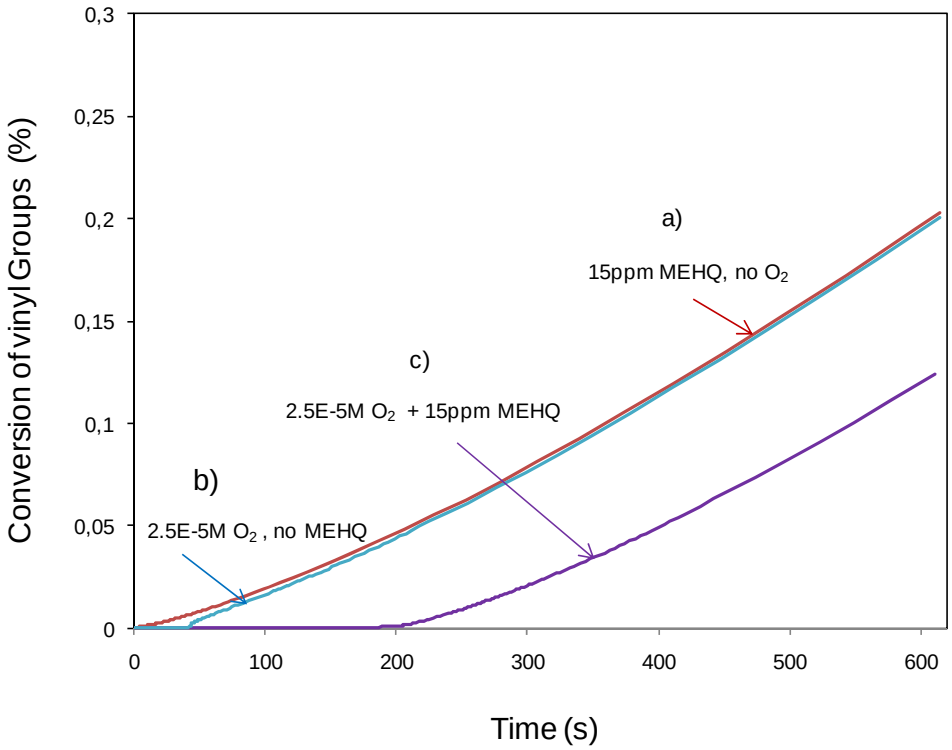

Figure 8: Simulation results comparing the vinyl group conversion over time in dosimeters with and without oxygen and MEHQ contamination. The simulated 6%T 50 %C dosimeters were irradiated at a dose rate of 1 Gy/min to a total dose of 10 Gy.